nature chemical biology

ARTICLE

PUBLISHED ONLINE: 7 JULY 2013 | DOI: 10.1038/NCHEMBIO.1290

Oxysterol binding to the extracellular domain of Smoothened in Hedgehog signaling

Daniel Nedelcu[1,2], Jing Liu[1,2], Yangqing Xu[1], Cindy Jao[1] & Adrian Salic[1]*

Oxysterols bind the seven-transmembrane protein Smo (Smo) and potently activate vertebrate Hedgehog (Hh) signaling, a pathway essential in embryonic development, adult stem cell maintenance and cancer. It is unknown, however, whether oxysterols are important for normal vertebrate Hh signaling and whether antagonizing oxysterols can inhibit the Hh pathway. We developed azasterols that block Hh signaling by binding the oxysterol-binding site of Smo. We show that the binding site for oxysterols and azasterols maps to the extracellular, cysteine-rich domain of Smo and is completely separable from the site bound by other small-molecule modulators, located within the heptahelical bundle of Smo. Smo mutants in which oxysterol binding is abolished no longer respond to oxysterols and cannot be maximally activated by the Hh ligand. Our results show that oxysterol binding to vertebrate Smo is required for normal Hh signaling and that targeting the oxysterol-binding site is an effective strategy to inhibit Smo.

Cell-cell signaling via the Hh pathway is critical for numerous aspects of metazoan embryonic development and regeneration, whereas excessive Hh activity is involved in many cancers[1,2]. Among poorly understood aspects of Hh signal transduction is the question of how Hh signals are relayed across the plasma membrane via the functional interaction between the multispanning membrane protein Patched (Ptch), which functions as the Hh receptor, and the seven-transmembrane protein Smo, a member of the Frizzled family of membrane proteins. In the absence of the Hh ligand, Ptch inhibits Smo through an unknown mechanism, ensuring that signals are not relayed to the cytoplasm. Hh signaling is initiated by binding of the Hh ligand to Ptch, leading to Smo activation and the consequent initiation of a specific transcriptional program driven by the Gli transcription factors.

The mechanism of Smo regulation during Hh signaling is currently unknown. Like other seven-transmembrane proteins, Smo equilibrates between active and inactive conformations, and it is thought that this equilibrium is controlled by a ligand[3] whose identity has remained elusive. Consistent with this hypothesis, vertebrate Smo harbors within its heptahelical bundle a binding site[4] (hereby 'Site A') reminiscent of G protein–coupled receptors. Site A is targeted by numerous small molecules, including Smo inhibitors (such as the alkaloid cyclopamine (Cyc)[4], SANT1 (ref. 5) or the US Food and Drug Administration–approved Smo inhibitor GDC0449 (ref. 6)) and activators (such as SAG[5,7] and purmorphamine[8]); however, no endogenous small molecule that binds Site A has been identified so far.

The only natural molecules that activate Smo are oxysterols, which are oxidized cholesterol derivatives with potent effects on many cellular processes, including signaling and metabolism. Vertebrate Hh signaling is stimulated by oxysterols carrying hydroxyl groups on the isooctyl side chain of the molecule[9,10], the most potent being 20(*S*)-hydroxycholesterol (20-OHC; **Fig. 1a**)[11,12]. Oxysterols activate Smo allosterically by binding a second site distinct from Site A[12] (hereby 'Site B'). Several important questions about the participation of oxysterols in Hh signaling are open. First, it is unknown where Site B is located in Smo and whether it is separable from Site A. Second, although Site A binds both Smo activators and inhibitors, we only know of oxysterol activators that bind Site B, raising the question of whether Site B can also be targeted by inhibitors. Finally, although oxysterols activate Smo, it is unknown whether their binding to Smo is required for Smo activation during normal Hh signaling.

We have developed azasterols that block Hh signaling triggered by the Hh ligand and by 20-OHC. These compounds compete with 20-OHC for binding Smo, indicating that they bind Site B; in contrast, azasterols do not compete with small molecules that bind Site A. We used azasterol and oxysterol affinity probes to map Site B to the extracellular, cysteine-rich domain (CRD) of vertebrate Smo (SmoCRD); furthermore, we show that Site A and B are completely separable. When Site B is mutated, 20-OHC binding to Smo is abolished, and 20-OHC can no longer activate Smo, thus functionally validating the unexpected identification of Site B within SmoCRD. These oxysterol-insensitive mutants have greatly decreased responsiveness to Hh compared to wild-type Smo, indicating that binding of endogenous oxysterols to Smo is necessary for high vertebrate Hh signaling.

RESULTS

A Hh inhibitor that mimics sterol depletion

20-OHC strongly activates vertebrate Hh signaling[11,12]; however, the consequences for Hh signaling of blocking 20-OHC are not known. To obtain a potential 20-OHC inhibitor, we synthesized 22-azacholesterol (22-NHC (**1**); **Fig. 1a**). When tested in Hh-responsive NIH-3T3 cells, 22-NHC inhibited signaling by Sonic Hedgehog (Shh) in a dose-dependent manner, with a half-maximum inhibitory concentration (IC_{50}) of about 3 μM (**Fig. 1b**); notably, cells exposed to up to 20 μM 22-NHC for 36 h did not show signs of toxicity. Synthesis of 22-NHC generates a C20 stereocenter, resulting in two possible diastereomers, 22(*S*)-NHC and 22(*R*)-NHC. Our synthesis generated predominantly 22(*S*)-NHC, and pure 22(*S*)-NHC recapitulated the inhibitory activity of the mix. 22-NHC did not affect the half-maximum effective concentration (EC_{50}) of Shh, but it decreased maximum stimulation (**Fig. 1b**), indicating noncompetitive inhibition.

We first sought to determine the step in Hh signal transduction inhibited by 22-NHC. Binding of Shh to Patched1 (Ptch1) causes its removal from primary cilia[13], which triggers Smo activation. 22-NHC had no effect on the disappearance of Ptch1

[1]Department of Cell Biology, Harvard Medical School, Boston, Massachusetts, USA. [2]These authors contributed equally to this work.
*e-mail: asalic@hms.harvard.edu

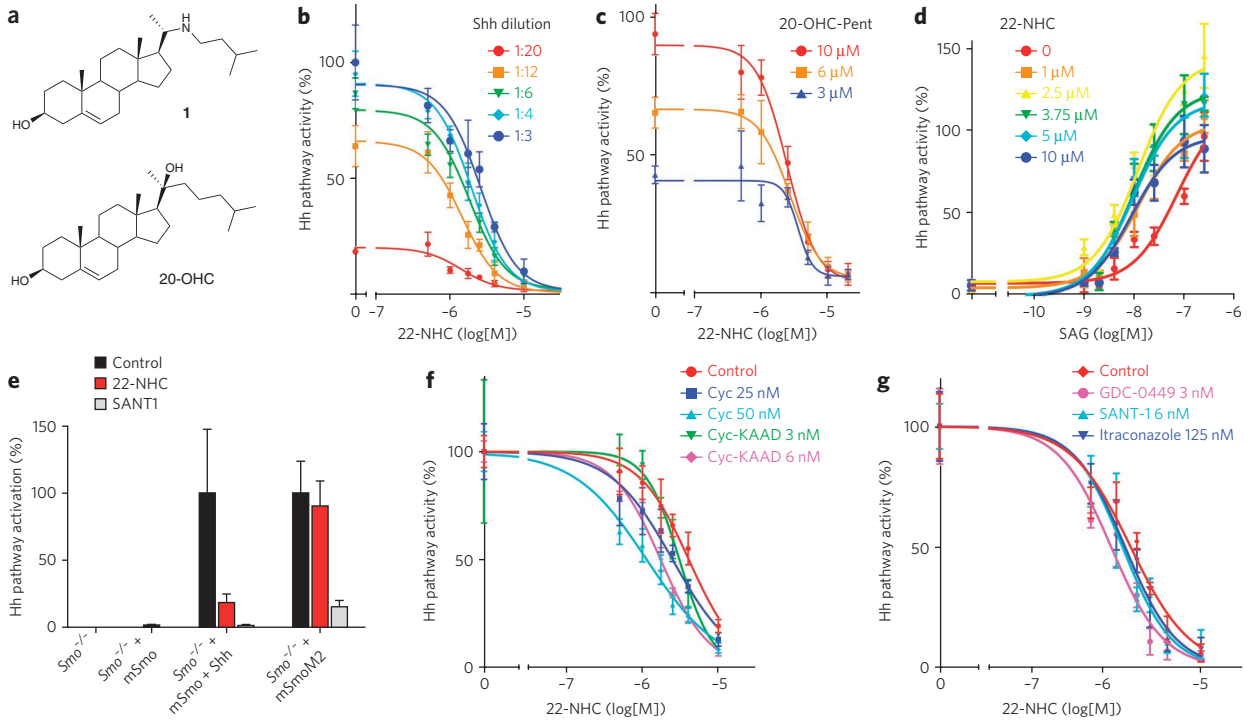

Figure 1 | 22-NHC inhibits vertebrate Hh signaling. (**a**) Structure of 22-NHC (**1**) and 20(*S*)-OHC. (**b**) Shh Light II cells were treated with various concentrations of Shh in the presence of increasing amounts of 22-NHC, and Hh pathway activation was measured by luciferase assay. 22-NHC inhibits Hh pathway activation by Shh but does not change the EC_{50} of Shh. (**c**) As in **b**, but Hh signaling was activated by various concentrations of the 20-OHC analog 20-OHC-Pent. 22-NHC inhibits Hh pathway activation by 20-OHC-Pent without changing the EC_{50}. (**d**) As in **b**, but Hh signaling was activated by various concentrations of SAG. 22-NHC does not inhibit Hh pathway activation by SAG, but it decreases the EC_{50} for SAG. For **b**–**d**, error bars represent s.d. (n = 4 independent experiments). (**e**) $Smo^{-/-}$ MEFs were rescued by stable expression of mSmo or the constitutively active mutant mSmoM2. Transcription of the Hh target gene, Gli1, was measured by quantitative PCR in the absence or presence of 22-NHC (20 μM) or SANT1 (2 μM). Error bars indicate s.d. (n = 3 independent experiments). 22-NHC does not inhibit SmoM2. (**f**) Shh Light II cells were stimulated with Shh in the presence of increasing amounts of 22-NHC, with the addition of Cyc or Cyc-KAAD. Hh pathway activity was assayed as in **b**. (**g**) As in **f**, but with addition of SANT1, GDC0449 or itraconazole. For **f** and **g**, error bars represent s.d. (n = 4 independent experiments).

from cilia in response to Shh (**Supplementary Results**, **Supplementary Fig. 1a**), suggesting that 22-NHC inhibits Hh signaling downstream of Ptch1.

We next asked whether 22-NHC inhibits two Smo activators, oxysterols and SAG. As our oxysterol we used 20-OHC-Pent (described below), a 20-OHC analog that we synthesized and that is slightly more potent than 20-OHC; similar results were obtained with 20-OHC. 22-NHC inhibited 20-OHC-Pent in a dose-dependent manner (**Fig. 1c**). 22-NHC did not change the EC_{50}, but it decreased the maximal stimulation by 20-OHC-Pent, indicating noncompetitive inhibition. In contrast, 22-NHC did not inhibit SAG (**Fig. 1d**); in fact, 22-NHC caused an increase in SAG responsiveness (the decreased EC_{50} for SAG in the presence of 22-NHC should be noted). Although we do not understand the basis for this increase, one possibility is that it is caused by 22-NHC promoting Smo translocation to cilia (described below), which might sensitize cells to SAG. Additionally, 22-NHC did not inhibit mSmoM2 (**Fig. 1e**), an oncogenic mouse Smo (mSmo) mutant locked in active conformation[14], or constitutive Hh signaling in $Sufu^{-/-}$ mouse embryonic fibroblasts (MEFs)[15] (**Supplementary Fig. 1b**), in which the Hh pathway is activated downstream of Smo. Together, these results indicate that 22-NHC targets either Smo or an unknown component between Ptch1 and Smo. The inhibition profile of 22-NHC mirrors the effect of sterol depletion, which blocks activation of the vertebrate Hh pathway by Shh but not by SAG or mSmoM2 or by loss of SuFu[16].

Finally, we asked whether 22-NHC synergizes with inhibitors of Smo. 22-NHC did not synergize with Cyc, Cyc-KAAD, SANT1, GDC0449 or itraconazole to inhibit Shh (**Fig. 1f**,**g**); conversely, these inhibitors did not affect the IC_{50} of 22-NHC. Thus 22-NHC does not interact with other Smo inhibitors, suggesting a different mechanism for 22-NHC.

22-NHC binds Smo at site distinct from Cyc

Shh stimulation causes rapid accumulation of Smo in primary cilia[17], a process blocked by some Site A Smo inhibitors, such as SANT1. We tested the possibility that 22-NHC inhibits this early event in Hh signaling. 22-NHC had no effect on Smo accumulation at cilia in response to Shh (**Supplementary Fig. 2a**), suggesting that 22-NHC can inhibit cilia-localized Smo. Notably, 22-NHC by itself caused ciliary accumulation of Smo (**Supplementary Fig. 2b**), although to a lesser extent than Shh (**Supplementary Fig. 2a**); this effect occurred rapidly, with ciliary Smo reaching maximum ciliary accumulation after a 3-h treatment with 22-NHC (**Supplementary Fig. 2c**). This behavior of 22-NHC is reminiscent of that of Cyc[18,19], a Hh inhibitor that binds Smo at Site A and causes Smo accumulation in cilia. To test whether 22-NHC also binds Site A, we performed binding assays in cells with the fluorescent derivative BODIPY-Cyc[4]. 22-NHC did not compete with binding of BODIPY-Cyc to mSmo, similarly to 20-OHC (**Supplementary Fig. 3a**); as expected, SANT1 abolished BODIPY-Cyc binding to Smo. We also synthesized a fluorescent derivative of SANT1, BODIPY-SANT1 (**Supplementary Fig. 3b**), which retains SANT1 activity (**Supplementary Fig. 3c**). 22-NHC did not compete with binding of BODIPY-SANT1 to mSmo, whereas SANT1 did (**Supplementary Fig. 3a**). Together, these results indicate that 22-NHC does not bind Site A of mSmo, in contrast to Cyc.

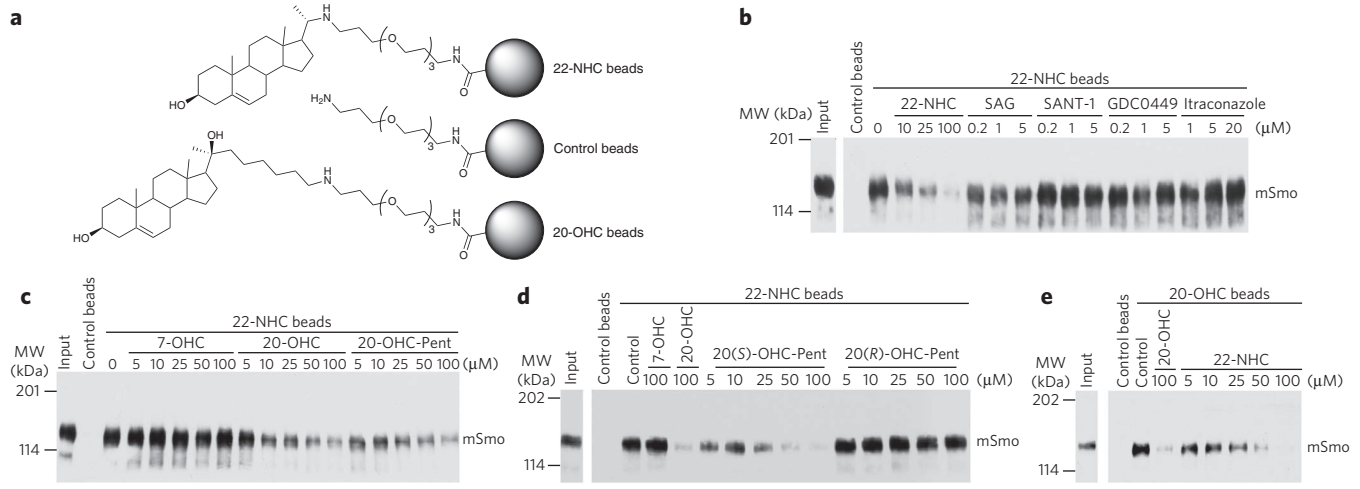

Figure 2 | 22-NHC binds Smo at the oxysterol-binding site. (**a**) Schematic of 22-NHC and 20-OHC affinity matrices. 22-NHC and 20-OHC are covalently attached to agarose beads via a PEG linker. Control beads carry only the PEG linker. (**b**) 22-NHC beads were incubated with detergent extracts of 293T cells expressing mSmo-Cherry in the presence of the indicated concentrations of competitor compounds. The beads were washed, and then bound protein was eluted, separated by SDS-PAGE and immunoblotted with Cherry-specific antibodies (anti-Cherry). A portion of the extract was analyzed in parallel to show input. mSmo specifically binds 22-NHC beads, and binding is not competed by other Smo inhibitors. MW, molecular weight. (**c**) As in **b**, but with the addition of the inactive oxysterol 7-OHC or the active oxysterols 20-OHC and 20-OHC-Pent. Binding of mSmo to 22-NHC beads is competed in a dose-dependent manner by 20-OHC and 20-OHC-Pent but not by 7-OHC. (**d**) As in **b** but with the addition of 20(*S*)-OHC-Pent and 20(*R*)-OHC-Pent. Binding of mSmo to 22-NHC beads is competed by the active *S* diastereomer but not by the inactive *R* diastereomer. (**e**) As in **b**, but using 20-OHC beads in the presence of free 22-NHC or 20-OHC. Binding of mSmo to 20-OHC beads is competed in a dose-dependent manner by free 22-NHC and 20-OHC. The full immunoblots for this figure are shown in **Supplementary Figure 11**.

To test whether 22-NHC binds mSmo at a different site, we developed a ligand affinity assay. We focused on the alkyl side chain of 22-NHC as a potential site for covalent attachment to beads and assayed analogs with modified side chains (**2**–**5**; **Supplementary Fig. 4a**). Analogs bearing N-propyl or N-ethyl groups retain the inhibitory activity of 22-NHC, albeit they are less potent (**Supplementary Fig. 4b**). Unexpectedly, C20 stereochemistry does not matter in these analogs: both *S* and *R* diastereomers inhibit Hh signaling, in contrast to the strict C20 stereochemistry required for Hh activation by oxysterols[12]. For analogs bearing N-hydroxypropyl or N-hydroxyethyl groups, the *S* diastereomers are modestly active, whereas the *R* diastereomers are inactive as Hh inhibitors (**Supplementary Fig. 4b**).

On the basis of the structure-function analysis above, we synthesized 22-NHC-PEG-NH_2 (**6**; **Supplementary Note**), a derivative with a PEG linker that was covalently attached to amine-reactive beads (**Fig. 2a**). As a source of mSmo protein, we used detergent extracts of 293T cells stably expressing mSmo tagged with mCherry; this fusion protein is active, rescuing Hh signaling in $Smo^{-/-}$ MEFs (described below). 22-NHC beads efficiently captured mSmo (**Fig. 2b**), preferentially the glycosylated species with low electrophoretic mobility, representing post-Golgi mSmo; this preference suggests that it is mainly mature mSmo that binds 22-NHC. Binding of mSmo to 22-NHC beads was competed in a dose-dependent manner by free 22-NHC added to the binding reaction (**Fig. 2b**), suggesting that it was specific. SAG, SANT1 and GDC0449 had no effect on mSmo binding to 22-NHC beads (**Fig. 2b**), consistent with 22-NHC not binding Site A. Itraconazole, a Smo inhibitor that does not bind Site A[20], also had no effect (**Fig. 2b**). As a negative control, we used beads derivatized with the PEG linker incorporated into 22-NHC-PEG-NH_2 (**Fig. 2a**); these beads captured negligible amounts of mSmo (**Fig. 2b**). As further proof of specificity, 22-NHC beads did not bind a seven-transmembrane protein related to Smo, mouse Frizzled-7 (mFz7; **Supplementary Fig. 5a**). Finally, binding was specific for vertebrate Smo: 22-NHC beads did not bind *Drosophila* Smo (DrSmo; **Supplementary Fig. 5a**), but they bound *Xenopus laevis* Smo (xSmo; **Supplementary Fig. 5b**). Together, these results demonstrate that 22-NHC binds vertebrate Smo at a site different from Site A and from the hypothetical itraconazole site.

22-NHC binds the oxysterol-binding site of Smo

Oxysterols are allosteric activators of Smo that bind Site B, which is distinct from Site A and the itraconazole site[12]. We investigated whether 22-NHC binds Smo at Site B by oxysterol competition experiments. Binding of mSmo to 22-NHC beads was competed in a dose-dependent manner by two active oxysterols, 20-OHC and 20-OHC-Pent, whereas 7-hydroxycholesterol (7-OHC), an inactive oxysterol[9], had no effect (**Fig. 2c**); similar results were obtained for xSmo (**Supplementary Fig. 5b**). Thus, 22-NHC and oxysterols that activate the Hh pathway compete for binding to vertebrate Smo.

Binding of 20-OHC is strictly stereospecific: 20(*S*)-OHC binds Smo, whereas 20(*R*)-OHC does not[12]. If 22-NHC binds Site B, it would be expected that oxysterol competition be also stereospecific. To test this prediction, we prepared pure diastereomers of 20-OHC-Pent (**Supplementary Fig. 5c**). Only the active diastereomer 20(*S*)-OHC-Pent (described below) competed mSmo binding to 22-NHC beads, whereas the inactive diastereomer 20(*R*)-OHC-Pent had no effect (**Fig. 2d**). Thus, oxysterol C20 stereochemistry is critical for competing with binding of 22-NHC to Smo.

To perform reciprocal binding experiments, we generated 20-OHC beads (**Fig. 2a**) using an amine derivative of 20-OHC that incorporates the same PEG linker used for 22-NHC beads. These 20-OHC beads bound mSmo (**Fig. 2e**), as described for a similar 20-OHC affinity matrix[12]. Notably, 22-NHC inhibited mSmo binding to 20-OHC beads in a dose-dependent manner (**Fig. 2e**). Like 22-NHC beads, 20-OHC beads did not bind DrSmo (**Supplementary Fig. 5d**), but they bound xSmo (**Supplementary Fig. 5e**), consistent with oxysterols activating the vertebrate but not the *Drosophila* Hh pathway. Furthermore, in a variety of Smo-binding experiments (described below), 22-NHC and 20-OHC beads behaved virtually identically. Together, these results indicate that 22-NHC and 20-OHC bind the same site (Site B) and suggest that 22-NHC inhibits Hh signaling by competing with binding of 20-OHC to mSmo.

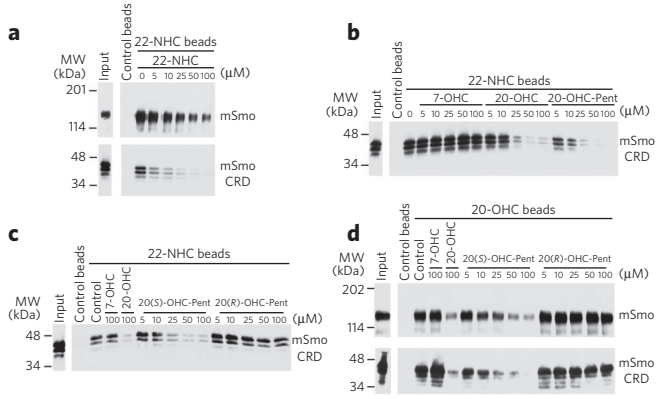

Figure 3 | Oxysterols and 22-NHC bind the extracellular CRD of vertebrate Smo. (**a**) Secreted hemagglutinin-tagged mSmoCRD and detergent extracts of 293T cells expressing mSmo-Cherry were tested for binding to 22-NHC beads in the presence of free 22-NHC. MSmoCRD binds 22-NHC beads, similarly to mSmo. MW, molecular weight. (**b**) mSmoCRD binding to 22-NHC beads was assayed as in **a** in the presence of 7-OHC, 20-OHC or 20-OHC-Pent. Only the active sterols 20-OHC and 20-OHC-Pent compete with mSmoCRD binding to 22-NHC beads, whereas the inactive 7-OHC does not. (**c**) As in **b**, but in the presence of the diastereomers 20(*S*)-OHC-Pent and 20(*R*)-OHC-Pent. Only the active *S* diastereomer competes with mSmoCRD binding to 22-NHC beads. (**d**) MSmoCRD and mSmo binding to 20-OHC beads was assayed as in **c**. Both mSmoCRD and mSmo bind 20-OHC beads and are competed by 20(*S*)-OHC-Pent but not 20(*R*)-OHC-Pent. The binding affinities of mSmoCRD and mSmo to 20-OHC beads are similar. The full immunoblots for this figure are shown in **Supplementary Figure 11**.

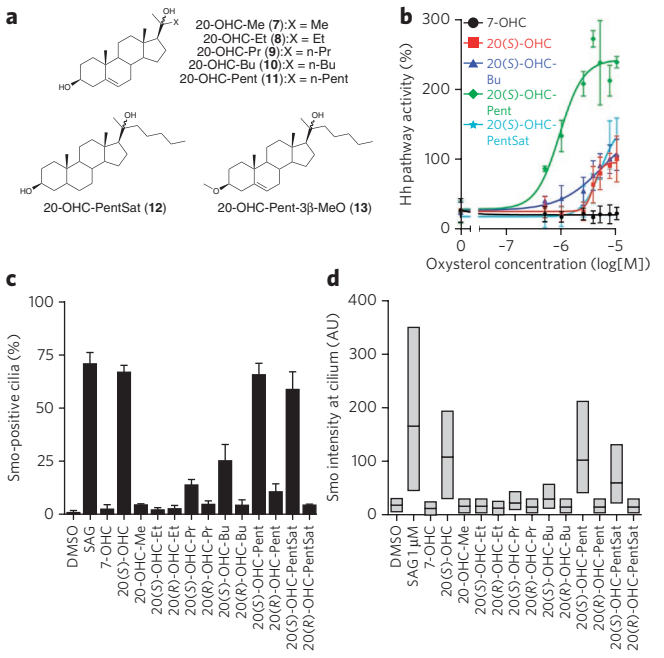

Figure 4 | Structural requirements for oxysterol activation of Smo. (**a**) Structures of 20-OHC analogs used in this study (**7**–**13**). All of the analogs except 20-OHC-Me (**7**) have a C20 stereocenter, and pure *S* and *R* diastereomers were isolated and assayed separately. (**b**) Shh Light II cells were treated with varying concentrations of the oxysterols 20(*S*)-OHC, 20(*S*)-OHC-Pent, 20(*S*)-OHC-PentSat and 20(*S*)-OHC-Bu, followed by measuring Hh pathway activity by luciferase assay. The inactive oxysterol, 7-OHC, was used as a negative control. Error bars represent s.d. ($n = 4$ independent experiments). (**c**) NIH-3T3 cells were incubated overnight with the indicated oxysterols (10 μM). Cells were then fixed and processed for immunofluorescence with rabbit anti-Smo (to detect endogenous Smo) and mouse anti-acetylated tubulin (to visualize primary cilia). SAG (1 μM) and 7-OHC (10 μM) were used as a positive and negative control, respectively. The graph shows the percentage of Smo-positive cilia. At least 150 cilia were analyzed per condition. Error bars represent the subsampling s.d. of the fraction of positive cilia (Online Methods). (**d**) As in **c**, but with box plots showing the fluorescence intensity of endogenous Smo at cilia. For each condition, the Smo signal was normalized to the intensity of the 20(*S*)-OHC treatment. The lower and upper bounds of each box represent the twenty-fifth and seventy-fifth percentile of the distribution of Smo intensity at cilia, and the horizontal line represents the median intensity across the entire population of cilia. AU, arbitrary units.

20-OHC and 22-NHC bind Smo extracellular domain

The location of Site B has not been determined, and it is unknown whether Site B and Site A are separable, particularly in view of their allosteric interaction. We used mSmo deletion analysis (**Supplementary Fig. 6a**) and 22-NHC and 20-OHC ligand affinity to map the location of Site B. MSmo lacking the extracellular CRD (mSmoΔCRD) did not bind 22-NHC beads (**Supplementary Fig. 6b**) or 20-OHC beads (**Supplementary Fig. 6c**), in contrast to full-length mSmo and mSmo lacking the intracellular C-terminal domain (mSmoΔICD) (**Supplementary Fig. 6d**). Notably, mSmoΔCRD bound BODIPY-Cyc (**Supplementary Fig. 7a**) and was functional in *Smo*$^{-/-}$ MEFs (described below), indicating that it was properly folded. These results show that the CRD is required for mSmo binding to 20-OHC and 22-NHC.

We next asked whether mSmoCRD, produced in cultured cells as a soluble, secreted protein, is sufficient to bind 22-NHC and 20-OHC. MSmoCRD bound 22-NHC beads, and binding was competed by free 22-NHC, similarly to full-length mSmo (**Fig. 3a**). Notably, secreted DrSmoCRD did not bind 22-NHC beads (**Supplementary Fig. 7b**), as expected from the lack of binding of DrSmo. Binding of mSmoCRD to 22-NHC beads was also competed by 20-OHC and 20-OHC-Pent but not by 7-OHC (**Fig. 3b**), suggesting that, like full-length mSmo, mSmoCRD binds oxysterols that activate Hh signaling. Furthermore, the stereochemistry of oxysterol competition was identical to that for mSmo: 20(*S*)-OHC-Pent but not 20(*R*)-OHC-Pent competed mSmoCRD binding to 22-NHC beads (**Fig. 3c**). We obtained identical results using 20-OHC beads. mSmoCRD bound 20-OHC beads with an affinity similar to that of mSmo and was competed by 20(*S*)-OHC-Pent but not by 20(*R*)-OHC-Pent (**Fig. 3d**). In addition, binding of mSmo and mSmoCRD to 20-OHC beads was competed by the active oxysterol 25-OHC but not by the inactive 7-ketocholesterol[9] (**Supplementary Fig. 7c**). Together, these results demonstrate that Site B resides in SmoCRD and is completely separable from Site A. Notably, it was proposed that SmoCRD might bind sterols on the basis of structural similarity between the sterol-binding protein NPC2 and the CRD of Frizzled proteins[21]; our findings confirm this prediction.

Oxysterol structural requirements in Hh signaling

To better understand the effect of oxysterols on Hh signaling, we asked which structural aspects of 20-OHC are important for mSmo activation and ciliary recruitment. We first focused on the isooctyl tail and synthesized 20-OHC analogs with progressively shorter tails (**Fig. 4a**). Shortening the tail by one or two carbons (20-OHC-Pent and 20-OHC-Bu) preserved activity (**Fig. 4b**). As for 20-OHC[12], the diastereomers 20(*S*)-OHC-Pent and 20(*S*)-OHC-Bu were active (**Fig. 4b**), whereas 20(*R*)-OHC-Pent and 20(*R*)-OHC-Bu were inactive (**Supplementary Fig. 8a**); this correlated with their ability to recruit mSmo to cilia (**Fig. 4c,d**). Analogs of 20-OHC with shorter tails (20-OHC-Pr, 20-OHC-Et and 20-OHC-Me) did not stimulate Hh signaling (**Supplementary Fig. 8a**), indicating that a tail of six carbon atoms is the minimum for mSmo activation.

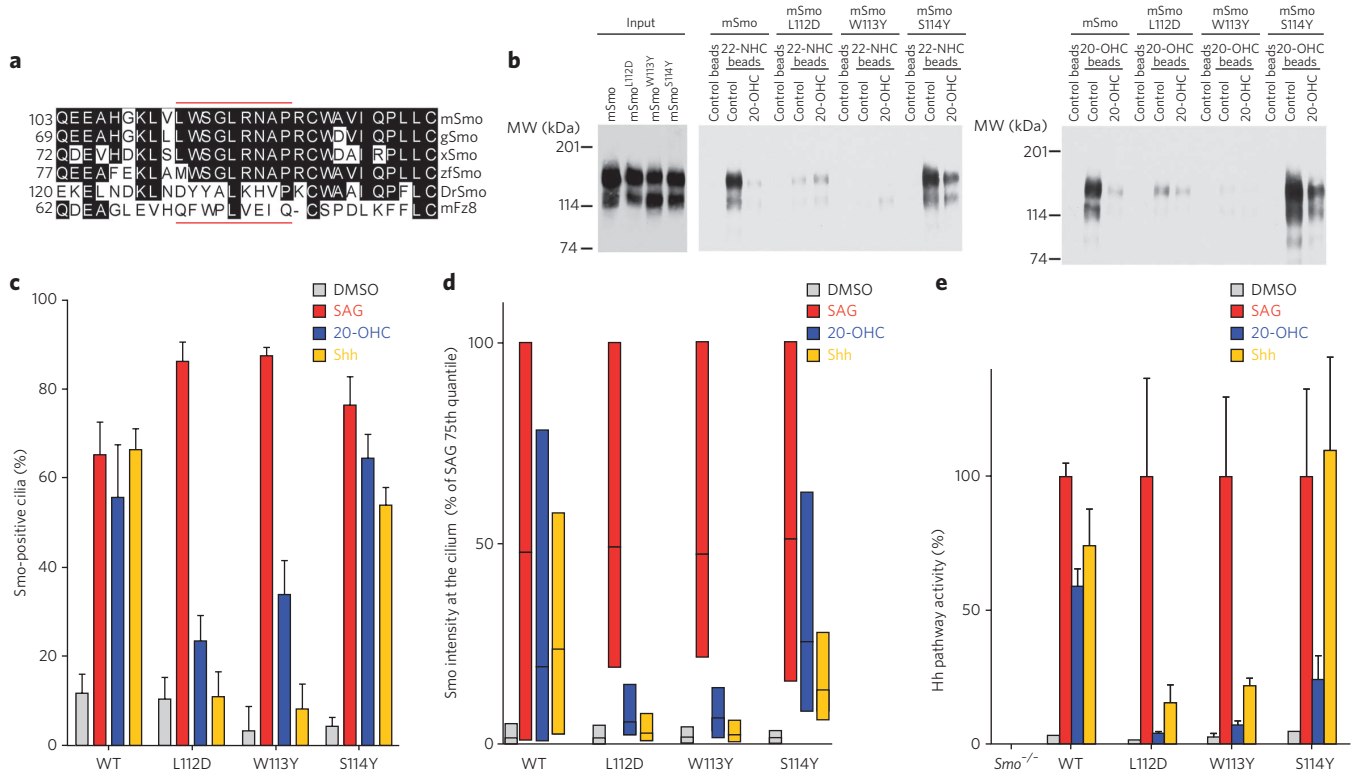

Figure 5 | Oxysterol binding to Smo is required for high Hh signaling. (**a**) Alignment of a portion of CRDs of mSmo, chicken Smo (gSmo), xSmo, zebrafish Smo (zfSmo), DrSmo and mFz8. The stretch indicated with red lines contains five residues that, in mFz8, contact the Xwnt8 palmityl moiety (Gln71, Phe72, Pro74, Leu75 and Ile78). (**b**) Cherry-tagged mSmo, mSmo^{L112D}, mSmo^{W113Y} and mSmo^{S114Y} were tested for binding to 22-NHC and 20-OHC beads, in the presence or absence of 20-OHC (100 μM). MSmo^{L112D} and mSmo^{W113Y} do not bind 22-NHC and 20-OHC beads. The full immunoblot is shown in **Supplementary Figure 11**. MW, molecular weight. (**c**) *Smo*$^{-/-}$ MEFs rescued with small amounts of mSmo, mSmo^{L112D}, mSmo^{W113Y} or mSmo^{S114Y} were incubated overnight with DMSO control, SAG (1 μM), 20-OHC (10 μM) or Shh. The graph shows the percentage of Smo-positive cilia. Error bars represent the subsampling s.d. of the fraction of positive cilia (Online Methods). Between 131 and 207 cilia were analyzed per condition. MSmo^{L112D} and mSmo^{W113Y} have a defective response to 20-OHC and Shh. (**d**) As in **c**, but with box plots showing Smo fluorescence intensity at cilia. For each condition, the Smo signal was normalized to the intensity of the SAG treatment for the respective cell line. (**e**) As in **c**, but cells were processed for quantitative PCR to measure Gli1 transcription. For each treatment, the amount of Gli1 was normalized to that induced by SAG in the respective cell line. Error bars show s.d. (n = 3 independent experiments). MSmo^{L112D} and mSmo^{W113Y} do not respond to 20-OHC and have a reduced responsiveness to Shh.

These shorter tail analogs did not inhibit pathway activation by Shh (**Supplementary Fig. 8b**). Notably, 20(*S*)-OHC-Pr caused accumulation of mSmo at cilia, whereas 20-OHC-Me, 20-OHC-Et (*R* and *S*) and 20(*R*)-OHC-Pr had no effect (**Fig. 4c**,**d**). Furthermore, 20(*S*)-OHC-Pr potentiated Shh activity (**Supplementary Fig. 8b**), an effect similar to the Shh sensitization observed with glucocorticoids that cause mSmo accumulation in cilia without activating transcription[22]. Thus, 20(*S*)-OHC-Pr is sufficient to localize mSmo to cilia, but it cannot activate it, suggesting that it induces a mSmo conformation distinct from the active one induced by analogs with longer tails.

Finally, we asked whether the Δ5 double bond and the 3β-OH group are important. The saturated analog, 20-OHC-PentSat (**Fig. 4a**), activated Hh signaling as the *S* diastereomer (**Fig. 4b**), whereas the *R* diastereomer was inactive (**Supplementary Fig. 8a**); thus, the Δ5 double bond is not required for activity. A 3β-methyl ether analog of 20-OHC-Pent (20-OHC-Pent-3β-OMe; **Fig. 4a**) did not activate or inhibit Hh signaling (**Supplementary Fig. 8c**) and had no effect on mSmo binding to 22-NHC beads (**Supplementary Fig. 8d**). These results indicate that a free 3β-OH group is absolutely required for 20-OHC activity.

Role of oxysterols in vertebrate Hh signaling

Although oxysterols activate Smo, it is not known what role their interaction with Smo has in Hh signaling. To generate mSmo mutants that do not bind oxysterols, we relied on the homology between the CRDs of Smo and Frizzled (Fz) proteins. It was proposed that SmoCRD binds sterols similarly to the way FzCRD binds the palmityl residue of Wnt proteins[21]. On the basis of the crystal structure of mFz8CRD bound to Xwnt8 (ref. 23), we focused on a stretch of eight amino acids in mSmo whose corresponding sequence in mFz8 includes five amino acids that form contacts with the palmityl residue[23] (**Fig. 5a**). This stretch is conserved among vertebrate Smo orthologs but not in DrSmo, which does not bind oxysterols. To test whether this stretch is important for oxysterol binding, we swapped amino acids 112–119 of mSmo for the corresponding amino acids of DrSmo. The resulting mSmo mutant (mSmo^{DrSmoCRDmut}) did not bind 22-NHC beads, (**Supplementary Fig. 9a**), whereas the secreted mSmoCRD^{DrSmoCRDmut} did not bind 20-OHC beads (**Supplementary Fig. 9b**). Notably, mSmo^{DrSmoCRDmut} bound BODIPY-Cyc (**Supplementary Fig. 9c**), indicating proper folding and an intact Site A.

To determine whether mSmo^{DrSmoCRDmut} and mSmoΔCRD respond to oxysterols, we generated *Smo*$^{-/-}$ MEFs that stably express small amounts of the proteins and assayed their activation by SAG and 20-OHC by immunofluorescence (to measure ciliary recruitment of mSmo; **Supplementary Fig. 9d**,**e**) and by quantitative PCR (to measure the transcriptional output of the Hh pathway; **Supplementary Fig. 9f**). Both mSmo^{DrSmoCRDmut} and mSmoΔCRD rescued the response of *Smo*$^{-/-}$ MEFs to SAG, indicating that they are fully functional in activating the downstream steps of Hh signaling.

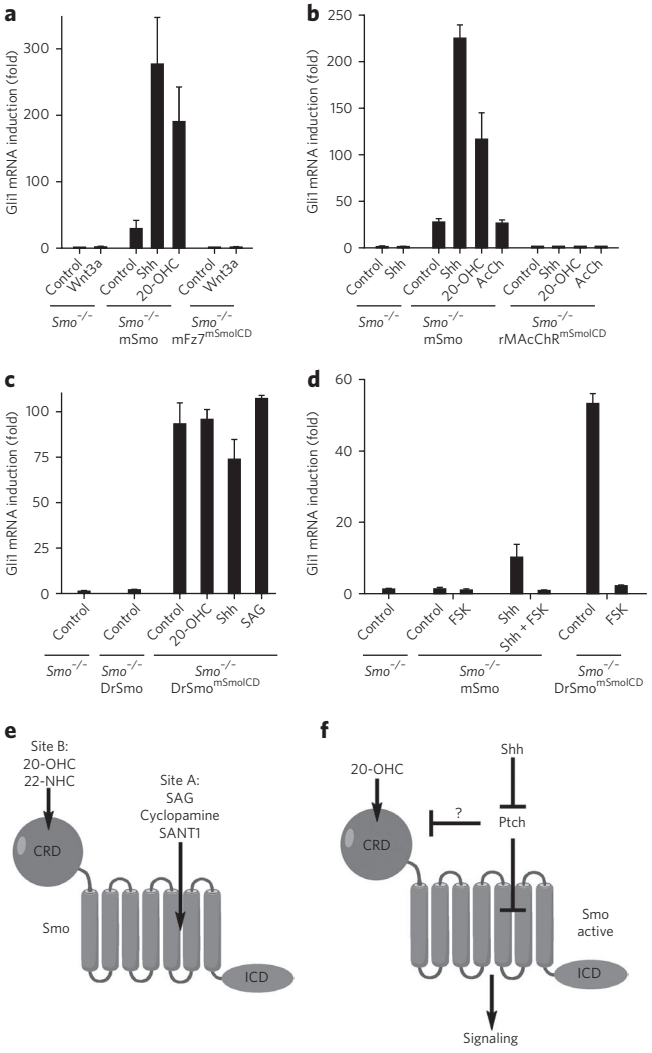

Figure 6 | Conserved and divergent aspects of Smo signaling. (**a**) *Smo*$^{-/-}$ MEFs, stably expressing mSmo or the cilia-localized chimera mFz7^{mSmoICD} were incubated with control medium, 20-OHC (10 μM), Shh or Wnt3a. The cells were processed for quantitative PCR to measure Gli1 transcription. Error bars show s.d. (n = 3 independent experiments). MFz7^{mSmoICD} did not rescue Hh signaling in *Smo*$^{-/-}$ cells, irrespective of the presence of Wnt3a. (**b**) As in **a**, but with stable expression of the chimera rMAcChR^{mSmoICD}, which is recruited to cilia by treatment with acetylcholine (AcCh, 100 μM). RMAcChR^{mSmoICD} does not rescue Hh signaling in the presence or absence of AcCh. (**c**) As in **a** but with stable expression of small amounts of DrSmo^{mSmoICD}. DrSmo^{mSmoICD} is constitutively active and is not further activated by 20-OHC (10 μM), Shh or SAG (400 nM). In contrast, DrSmo is inactive in *Smo*$^{-/-}$ MEFs. (**d**) As in **c**, but with addition of 20 μM forskolin (FSK) to block Hh signaling downstream of Smo. Signaling by both mSmo and DrSmo^{mSmoICD} is blocked by FSK. (**e**) Schematic of the mSmo protein and of the location of Sites A and B. For each site, activators (SAG for Site A and 20-OHC for Site B) and inhibitors (cyclopamine and SANT1 for Site A and 22-NHC for Site B) are indicated. (**f**) Regulation of vertebrate Smo. Inhibition of Ptch by Shh results in Smo Site A activation; it is unclear whether Site B is also activated by Shh. The oxysterol 20-OHC, which binds to Site B in the extracellular domain of Smo, potentiates Site A activation. Active Smo then signals to the cytoplasm.

However, mSmo^{DrSmoCRDmut} and mSmoΔCRD did not respond to 20-OHC, in contrast to mSmo. These results validate our mapping of the oxysterol-binding site within mSmoCRD.

We identified two mSmo point mutants defective in oxysterol binding by individually mutating residues in the Leu-Trp-Ser sequence (amino acids 112–114) to the corresponding Asp-Tyr-Tyr sequence in DrSmo. mSmo^{L112D} and mSmo^{W113Y} no longer bound 22-NHC and 20-OHC beads, in contrast to mSmo^{S114Y} and mSmo (**Fig. 5b**). Notably, mSmo^{L112D} and mSmo^{W113Y} showed a prominent post-Golgi band on SDS-PAGE (**Fig. 5b**) and bound BODIPY-Cyc (**Supplementary Fig. 9g**), indicating proper folding.

To test the function of oxysterol binding to mSmo, we compared Hh signaling in *Smo*$^{-/-}$ MEFs stably expressing mSmo, mSmo^{L112D}, mSmo^{W113Y} or mSmo^{S114Y} (**Fig. 5c–e**). As expected, all four of the proteins rescued the response to SAG. Consistent with loss of oxysterol binding, mSmo^{L112D} and mSmo^{W113Y} did not respond to 20-OHC, in contrast to mSmo and mSmo^{S114Y}. Remarkably, mSmo^{L112D} and mSmo^{W113Y} had a greatly reduced response to Shh compared to mSmo and mSmo^{S114Y}. Similarly, a lower response to Shh was observed for mSmoΔCRD (**Supplementary Fig. 9h,i**) and for the double mutant mSmo$^{L112D\ W113Y}$ (**Supplementary Fig. 9j**). In conclusion, binding of oxysterols to the CRD is required for high mSmo activation by Shh. In contrast, low mSmo activation by Shh still occurs in the absence of oxysterol binding. This suggests that Hh signaling controls mSmo via Site A or possibly via both Site A and Site B.

Conservation and divergence in Smo regulation

In spite of Smo conservation, only vertebrate Smo binds oxysterols, raising the question of whether Smo regulation is conserved. To begin addressing this issue, we asked whether DrSmo retains any signaling activity in vertebrate cells. When stably expressed in *Smo*$^{-/-}$ MEFs, DrSmo did not localize to cilia (**Supplementary Fig. 10a**) and was thus inactive (**Supplementary Fig. 10b**). This result was not surprising, as cilia are not involved in Hh signaling in *Drosophila*.

To direct DrSmo to cilia, we examined the ciliary localization determinants of mSmo. Because mSmoΔICD does not localize to cilia[24], we tested whether mSmoICD is sufficient for ciliary localization. We generated chimeras in which mSmoICD replaced the cytoplasmic tail of two seven-transmembrane proteins that do not traffic to cilia, mFz7 and the rat muscarinic acetylcholine receptor M2 (rMAChR). Stably expressed mFz7^{mSmoICD} localized to cilia in *Smo*$^{-/-}$ MEFs (**Supplementary Fig. 10c**), whereas rMAChR^{mSmoICD} did not but was strongly recruited to cilia by treatment with either agonist (acetylcholine) or antagonist (scopolamine) (**Supplementary Fig. 10c**). We interpret this behavior of rMAChR^{mSmoICD} as a result of improved folding due to agonist or antagonist binding. Both mFz7^{mSmoICD} and rMAChR^{mSmoICD} were inactive in Hh signaling, even in the presence of agonists Wnt3a (**Fig. 6a**) and acetylcholine, respectively (**Fig. 6b**). These results show that mSmoICD is sufficient for ciliary localization but not for activating Hh signaling.

To determine whether DrSmo can signal at cilia, we generated a chimera (DrSmo^{mSmoICD}) that consists of the DrSmo CRD and heptahelical bundle followed by mSmoICD. As expected, DrSmo^{mSmoICD} localized to cilia in *Smo*$^{-/-}$ MEFs (**Supplementary Fig. 10d**). Notably, DrSmo^{mSmoICD} strongly activated Hh signaling (**Fig. 6c**), indicating that the DrSmo portion of the chimera is active in vertebrate cells. DrSmo^{mSmoICD} was constitutively active and could not be further stimulated by 20-OHC, SAG or Shh (**Fig. 6c**); it was, however, inhibited by forskolin, which blocks Hh signaling downstream of Smo (**Fig. 6d**). The lack of response to 20-OHC and SAG is consistent with DrSmo^{mSmoICD} not binding these two molecules. The inability of Shh to stimulate DrSmo^{mSmoICD} indicates that mouse Ptch cannot repress DrSmo^{mSmoICD} at cilia, thus suggesting that DrSmo is regulated differently from mSmo. Finally, in contrast to mSmo, DrSmo^{mSmoICD} was not inhibited by sterol depletion (**Supplementary Fig. 10e,f**), indicating that oxysterols are not required for DrSmo^{mSmoICD} activation.

DISCUSSION

Our findings suggest a mechanism for how the vertebrate Hh pathway is modulated by oxysterols. During Hh signaling, Shh relieves

the inhibition exerted by Ptch on Smo, and an open question is how Smo is regulated. Endogenous small molecules are hypothesized to control the equilibrium between the active and the inactive conformation of Smo[3], in turn determining the output of Hh signaling at the membrane. Oxysterols[9,10], particularly 20-OHC[11,12], are so far the only metabolites that activate Hh signaling, acting as Smo allosteric activators[12]. We describe 22-NHC, a Hh inhibitor that acts by a new mechanism, namely, by competing with 20-OHC binding to Smo. 22-NHC inhibits Shh noncompetitively, consistent with 22-NHC binding the allosteric Smo Site B. To our surprise, Site B maps to the extracellular CRD of Smo, and we show that it is completely separable from Site A (**Fig. 6e**). We demonstrate that 20-OHC binding to SmoCRD is required for high Smo activation. Notably, Shh can still activate Smo mutants lacking a functional Site B, although it does so to a greatly reduced extent; thus, Site A is sufficient for Smo to respond to Shh. These results suggest that during Hh signaling, Smo is activated by two synergistic inputs: Shh-Ptch–dependent activation of Site A and allosteric activation by oxysterol binding to Site B (**Fig. 6f**). Many aspects of this mechanism remain to be deciphered, such as measuring endogenous 20-OHC, elucidating its biosynthesis and determining whether 20-OHC binding to Site B is controlled by Shh-Ptch or whether it represents an independent input.

Mapping the 20-OHC–binding site to SmoCRD confirms the prediction that Frizzled-type CRDs are related to sterol-binding proteins such as the lysosomal cholesterol carrier NPC2 (ref. 21). We used the crystal structure of the mFz8–Xwnt8 complex[23] to mutate mSmoCRD residues that align with mFz8CRD residues that bind the palmityl residue on Xwnt8. These mSmo mutants were defective in 20-OHC binding, suggesting that mSmoCRD-oxysterol binding most likely resembles mFz8CRD binding to palmitate; structural studies will be needed to determine exactly how SmoCRD binds 20-OHC. Remarkably, for two other sterol-binding membrane proteins, the sterol-binding sites also map to soluble portions: the Niemann-Pick protein 1 binds oxysterols via its N-terminal domain projecting in the lysosomal lumen[25], and the SREBP cleavage-activating protein binds cholesterol via a large endoplasmic reticulum luminal loop[26]. It will be important to determine whether sterol binding by soluble domains is a general feature among sterol-binding membrane proteins.

An important question is how Sites A and B of Smo are regulated during Hh signaling. No endogenous small molecule that binds Site A is known, and it is unclear whether such a molecule would be an agonist (which Ptch would prevent from reaching Smo) or antagonist (which Ptch would deliver to Smo). Our results indicate that Ptch controls Smo at least in part through Site A, but they cannot distinguish between these two alternatives. The situation is clearer for Site B, which, during Hh signaling, needs be occupied by an endogenous activator such as 20-OHC. This conclusion is based on the inhibitory effects of sterol depletion and blocking 20-OHC binding to Smo. The endogenous concentration of oxysterols such as 20-OHC is unknown, but it is most likely much lower than the micromolar EC_{50} for Hh activation. Although higher local concentrations might exist in cells, endogenous oxysterol concentrations are perhaps too low to activate Smo by themselves but are high enough to synergize with Site A activation by an endogenous agonist. One advantage of such a mechanism is that it allows a Shh-independent way to modulate signaling while ensuring that activation remains dependent on Shh-Ptch. Different tissues might have different oxysterol amounts and profiles, thus allowing for varying degrees of Hh signaling. Alternatively, in some cells, oxysterols might reach concentrations at which they activate Hh signaling in a ligand- or Ptch-independent manner, a possibility with important implications in cancer. Whole-animal studies will be important in determining whether the Hh pathway is differentially modulated by oxysterols in various tissues.

Another important question is how the allosteric interaction between Sites B and A result in Smo activation. It seems likely that SmoCRD binds 20-OHC, and the resulting complex interacts with the heptahelical bundle of Smo, contributing to stabilizing the active conformation of Site A. An active Site A is required for oxysterols to stimulate Hh signaling, as Site A inhibitors such as Cyc and SANT1 inhibit oxysterols[9,10,12]. SmoCRD, however, is not required for Smo activation by synthetic agonists such as SAG that bind Site A, suggesting that Site B has only a modulating role during Shh stimulation. Perhaps endogenous activation of Site A is weaker than that elicited by SAG, and thus oxysterols are required for high Smo activation. Detailed biochemical and structural studies will be needed to determine how the interaction between Sites A and B controls Smo activity.

The azasterol 22-NHC represents the first Site B inhibitor of Smo. 22-NHC inhibits Smo activated by Shh and 20-OHC but not by SAG, and it cannot inhibit the constitutively active SmoM2 mutant. Thus 22-NHC recapitulates the inhibitory effect of sterol depletion and of cholesterol biosynthesis defects on vertebrate Hh signaling[16]. The simplest interpretation is that sterol depletion removes the endogenous activator of Site B, which is perhaps 20-OHC. It should be pointed out that blocking HMG-CoA reductase with statins without also depleting sterols does not block Hh signaling[16], and thus the effect of 22-NHC is not explained by general inhibition of cholesterol biosynthesis. We cannot exclude the possibility that, in addition to binding Smo, 22-NHC might also block conversion of cholesterol into an unknown metabolite, such as an oxysterol.

Unlike vertebrate Smo, no small molecules are known that bind DrSmo. Furthermore, we found that DrSmo does not bind oxysterols and is not inhibited by sterol depletion. This raises the question of how DrSmo is activated and whether the activation mechanism is conserved. We assayed the activity of a portion of DrSmo consisting of the CRD and heptahelical bundle in mammalian cells after targeting it to cilia by fusion with the mSmoICD. This DrSmo construct is active and refractory to inhibition by Ptch, suggesting that DrSmo might be regulated differently from vertebrate Smo, in spite of Ptch conservation. Notably, DrSmoΔCRD is completely inactive in *Drosophila*[27], in contrast to vertebrate SmoΔCRD[3,28]. Thus, DrSmoCRD does not bind sterols but is absolutely required for function, perhaps because it has a critical role in stabilizing the active conformation of DrSmo. Understanding the mechanistic basis for the seeming evolutionary divergence in Smo regulation is an important future goal.

Received 14 March 2013; accepted 5 June 2013;
published online 7 July 2013

METHODS

Methods and any associated references are available in the online version of the paper.

References

1. Lum, L. & Beachy, P.A. The Hedgehog response network: sensors, switches, and routers. *Science* **304**, 1755–1759 (2004).
2. Ingham, P.W. & McMahon, A.P. Hedgehog signaling in animal development: paradigms and principles. *Genes Dev.* **15**, 3059–3087 (2001).
3. Taipale, J., Cooper, M.K., Maiti, T. & Beachy, P.A. Patched acts catalytically to suppress the activity of Smoothened. *Nature* **418**, 892–897 (2002).
4. Chen, J.K., Taipale, J., Cooper, M.K. & Beachy, P.A. Inhibition of Hedgehog signaling by direct binding of cyclopamine to Smoothened. *Genes Dev.* **16**, 2743–2748 (2002).
5. Frank-Kamenetsky, M. *et al.* Small-molecule modulators of Hedgehog signaling: identification and characterization of Smoothened agonists and antagonists. *J. Biol.* **1**, 10 (2002).
6. Robarge, K.D. *et al.* GDC-0449—a potent inhibitor of the hedgehog pathway. *Bioorg. Med. Chem. Lett.* **19**, 5576–5581 (2009).
7. Chen, J.K., Taipale, J., Young, K.E., Maiti, T. & Beachy, P.A. Small molecule modulation of Smoothened activity. *Proc. Natl. Acad. Sci. USA* **99**, 14071–14076 (2002).
8. Sinha, S. & Chen, J.K. Purmorphamine activates the Hedgehog pathway by targeting Smoothened. *Nat. Chem. Biol.* **2**, 29–30 (2006).

9. Dwyer, J.R. *et al.* Oxysterols are novel activators of the hedgehog signaling pathway in pluripotent mesenchymal cells. *J. Biol. Chem.* **282**, 8959–8968 (2007).
10. Corcoran, R.B. & Scott, M.P. Oxysterols stimulate Sonic hedgehog signal transduction and proliferation of medulloblastoma cells. *Proc. Natl. Acad. Sci. USA* **103**, 8408–8413 (2006).
11. Kim, W.K., Meliton, V., Amantea, C.M., Hahn, T.J. & Parhami, F. 20(*S*)-hydroxycholesterol inhibits PPARγ expression and adipogenic differentiation of bone marrow stromal cells through a hedgehog-dependent mechanism. *J. Bone Miner. Res.* **22**, 1711–1719 (2007).
12. Nachtergaele, S. *et al.* Oxysterols are allosteric activators of the oncoprotein Smoothened. *Nat. Chem. Biol.* **8**, 211–220 (2012).
13. Rohatgi, R., Milenkovic, L. & Scott, M.P. Patched1 regulates hedgehog signaling at the primary cilium. *Science* **317**, 372–376 (2007).
14. Taipale, J. *et al.* Effects of oncogenic mutations in Smoothened and Patched can be reversed by cyclopamine. *Nature* **406**, 1005–1009 (2000).
15. Svärd, J. *et al.* Genetic elimination of Suppressor of fused reveals an essential repressor function in the mammalian Hedgehog signaling pathway. *Dev. Cell* **10**, 187–197 (2006); erratum **10**, 409.
16. Cooper, M.K. *et al.* A defective response to Hedgehog signaling in disorders of cholesterol biosynthesis. *Nat. Genet.* **33**, 508–513 (2003).
17. Corbit, K.C. *et al.* Vertebrate Smoothened functions at the primary cilium. *Nature* **437**, 1018–1021 (2005).
18. Wang, Y., Zhou, Z., Walsh, C.T. & McMahon, A.P. Selective translocation of intracellular Smoothened to the primary cilium in response to Hedgehog pathway modulation. *Proc. Natl. Acad. Sci. USA* **106**, 2623–2628 (2009).
19. Rohatgi, R., Milenkovic, L., Corcoran, R.B. & Scott, M.P. Hedgehog signal transduction by Smoothened: pharmacologic evidence for a 2-step activation process. *Proc. Natl. Acad. Sci. USA* **106**, 3196–3201 (2009).
20. Kim, J. *et al.* Itraconazole, a commonly used antifungal that inhibits Hedgehog pathway activity and cancer growth. *Cancer Cell* **17**, 388–399 (2010).
21. Bazan, J.F. & de Sauvage, F.J. Structural ties between cholesterol transport and morphogen signaling. *Cell* **138**, 1055–1056 (2009).
22. Wang, Y. *et al.* Glucocorticoid compounds modify smoothened localization and hedgehog pathway activity. *Chem. Biol.* **19**, 972–982 (2012).
23. Janda, C.Y., Waghray, D., Levin, A.M., Thomas, C. & Garcia, K.C. Structural basis of Wnt recognition by Frizzled. *Science* **337**, 59–64 (2012).
24. Dorn, K.V., Hughes, C.E. & Rohatgi, R.A. Smoothened–Evc2 complex transduces the Hedgehog signal at primary cilia. *Dev. Cell* **23**, 823–835 (2012).
25. Infante, R.E. *et al.* Purified NPC1 protein: II. Localization of sterol binding to a 240-amino acid soluble luminal loop. *J. Biol. Chem.* **283**, 1064–1075 (2008).
26. Motamed, M. *et al.* Identification of luminal Loop 1 of Scap protein as the sterol sensor that maintains cholesterol homeostasis. *J. Biol. Chem.* **286**, 18002–18012 (2011).
27. Nakano, Y. *et al.* Functional domains and sub-cellular distribution of the Hedgehog transducing protein Smoothened in *Drosophila*. *Mech. Dev.* **121**, 507–518 (2004).
28. Aanstad, P. *et al.* The extracellular domain of Smoothened regulates ciliary localization and is required for high-level Hh signaling. *Curr. Biol.* **19**, 1034–1039 (2009).

Acknowledgments

We thank Y. Kishi and members of his laboratory for help with chiral chromatography and R. Rohatgi (Stanford University) for the initial gift of 20-OHC beads. A.S. is supported in part by US National Institutes of Health grant RO1 GM092924.

Author contributions

D.N. and A.S. performed cellular and biochemical experiments. J.L., C.J. and A.S. designed and synthesized reported compounds. J.L. purified and characterized the compounds. Y.X. and D.N. developed automated image analysis software, and D.N. analyzed imaging data. All authors contributed data to the manuscript. A.S. wrote the manuscript, with input from all other authors.

Competing financial interests

The authors declare no competing financial interests.

Additional information

Supplementary information and chemical compound information is available in the online version of the paper. Reprints and permissions information is available online at http://www.nature.com/reprints/index.html. Correspondence and requests for materials should be addressed to A.S.

ONLINE METHODS

Cell culture and reagents. The following compounds were obtained from commercial sources: cyclopamine from LC Laboratories (>99%); BODIPY-cyclopamine from Toronto Research Chemicals; SAG from Axxora (≥98%); forskolin from Sigma (≥98%); itraconazole from Sigma (≥98%); SANT1 from Calbiochem (≥95%); GDC0449 from LC Laboratories (>99%); 20-hydroxycholesterol, 7-hydroxycholesterol, 25-hydroxycholesterol and 7-ketocholesterol from Steraloids (≥98%).

Chemical synthesis. A complete description of the synthesis and characterization of sterol derivatives and BODIPY-SANT1 is provided in the **Supplementary Note**.

Antibodies. Polyclonal antibodies against Cherry and GFP were generated in rabbits (Cocalico Biologicals) and were affinity purified against recombinant GFP and Cherry immobilized on Affigel-10 beads (BioRad). Polyclonal rabbit anti-Smo were described before[29]. All of the polyclonal antibodies were used at a final concentration of 1–2 μg/mL. Mouse monoclonal anti–acetylated tubulin was obtained from Sigma (clone 6-11B-11) and was used at a 1:5,000 dilution for immunofluorescence. Rat monoclonal anti-HA was obtained from Roche (clone 3F10) and was used at a 1:1,000 dilution for immunoblotting.

DNA constructs. Expression constructs were assembled by PCR in the mammalian expression vector pCS2+, from which they were subcloned into a vector for lentiviral production[30]. Constructs encoding membrane proteins were tagged with Cherry at their C terminus. These constructs were: full-length mSmo, full-length *Drosophila* Smo (DrSmo), full-length mouse Frizzled7 (mFz7), mSmoΔICD (amino acids 1–554 of mSmo), mSmoM2 (constitutively active point mutant W539L), mSmoΔCRD (amino acids 183–793 of mSmo, preceded by the signal sequence of human calreticulin), DrSmo^{mSmoICD} (amino acids 1–556 of DrSmo fused to amino acids 543–793 of mSmo), mSmo^{DrSmoCRDmut} (amino acids 112–119 of mSmo, LWSGLRNA, replaced by amino acids 129–136 of DrSmo, DYYALKHV), mSmo^{L112D}, mSmo^{W113Y}, mSmo^{S114Y}, mSmo$^{L112D\,W113Y}$, mFz7^{mSmoICD} (amino acids 1–548 of mouse Frizzled7 fused to amino acids 543–793 of mSmo), rMAChR^{mSmoICD} (amino acids 1–442 of the rat muscarinic acetylcholine receptor M2 fused to amino acids 543–793 of mSmo). Full-length *Xenopus* Smo (xSmo) was tagged with eGFP at the C terminus and was expressed in Sf9 cells by baculoviral infection. The baculovirus was generated using the Bac-to-bac system (Life Sciences), according to the manufacturer's instructions. Constructs for expressing secreted extracellular CRDs of Smo proteins contained the signal sequence of human calreticulin, followed by the CRD sequence lacking the Smo signal sequence, followed by a hemagglutinin (HA) tag and eight histidine residues. The CRD sequences were: mSmoCRD (amino acids 32–236 of mSmo), DrSmoCRD (amino acids 32–257 of DrSmoSmo) and mSmoCRD^{DrSmoCRDmut} (amino acids 32–236 of mSmo^{DrSmoCRDmut}).

Cell culture and generation of stable cell lines. NIH-3T3 and Shh Light II cells were grown in Dulbecco's Modified Eagle's Medium (DMEM) supplemented with 10% bovine calf serum, penicillin and streptomycin. Mouse embryonic fibroblasts (MEFs) and 293T cells were grown in DMEM with 10% FBS, penicillin and streptomycin. Stable cell lines were generated by lentiviral transduction, followed by selection with blasticidin, as described[30]. *Smo*$^{-/-}$ MEFs expressing low amounts of various Cherry-tagged Smo proteins were isolated by fluorescence-activated cell sorting. Expression of the tagged construct was confirmed by immunofluorescence and by quantitative PCR assays of Hh pathway activity.

Hh ligand production. Hh ligand was produced by transiently transfecting 293T cells with an expression plasmid encoding amino acids 1–198 of human Shh. Shh was collected for 48 h into starvation medium (DMEM supplemented with penicillin and streptomycin). For maximal stimulation of the Hh pathway, Shh-conditioned medium was used diluted 1:3–1:4 into fresh starvation medium.

Reporter assays. Hh activity assays were performed in Shh Light II cells[14] (obtained from ATCC), a line of NIH-3T3 cells expressing firefly luciferase from a Gli-responsive promoter and *Renilla* luciferase from a constitutive promoter[14]. Confluent Shh Light II cultures were starved overnight in DMEM. The medium was then replaced with DMEM supplemented with the appropriate Hh pathway agonist, antagonist and/or test compound. All of the small molecules were added to cellular medium from concentrated stocks in DMSO, except 20-OHC-Pent-3β-MeO, which was added as a soluble complex with methyl-β-cyclodextrin (MCD), prepared as described[31]. After 30 h, the amount of Renilla and firefly luciferase was measured using the Dual-Glo kit (Promega). Hh pathway activity was expressed as the ratio of firefly to Renilla luciferase, normalized to 100% for maximally stimulated cells (cells treated with 1 μM SAG, 10 μM oxysterol, or 1:3 Shh ligand, depending on the experiment) or normalized to 1 for unstimulated cells. For all of the reporter assays, each data point represents the mean from quadruplicate wells of Shh Light II cells, and error bars represent the s.d. All of the experiments in the paper were performed at least twice. Dose-response curves were plotted using Prism (GraphPad), by nonlinear regression to a four-parameter curve.

Real-time PCR assays of the Hh pathway. Confluent NIH-3T3 cells or MEFs were starved overnight in starvation medium, after which they were incubated for 24 h in starvation medium supplemented with the desired compounds. Total RNA was isolated from cells with RNA-Bee (TelTest), treated with RNase-free DNase (Promega) and purified using the GenCatch total RNA Extraction System (Epoch Biolabs). Reverse transcription was performed using random hexamers and Transcriptor reverse transcriptase (Roche). Transcription of the Hh target gene *Gli1* was measured by real-time PCR using FastStart SYBR Green Master reagent (Roche) on a Rotor-Gene 6000 (Corbett Robotics). Relative gene expression was calculated using a Two Standard Curve method in which the gene of interest was normalized to the *ribosomal protein L27* (*RPL27*) gene. The sequences for gene-specific primers are: *RPL27*, 5′-GTCGAGATGGGCAAGTTCAT-3′ and 5′-GCTTGGCGATCTTCTTCTTG-3′; *Gli1*, 5′-GGCCAATCACAAGTCA AGGT-3′ and 5′-TTCAGGAGGAGGGTACAACG-3′. For all of the real-time PCR experiments, each data point represents the mean from triplicate wells of cultured cells, and error bars represent the s.d.

Immunofluorescence. Cells were grown on glass coverslips and were fixed in PBS with 4% formaldehyde, followed by permeabilization with TBST. Nonspecific binding sites were blocked by incubation in TBST with 50 mg/mL bovine serum albumin (TBST-BSA). Primary and secondary antibodies were used diluted in TBST-BSA. The primary antibodies were: polyclonal rabbit anti-Cherry (final concentration 2 μg/mL), polyclonal rabbit anti-mSmo[29] (final concentration 2 μg/mL), monoclonal mouse anti–acetylated tubulin (Sigma, clone 6-11B-11, final dilution of 1:5,000). Alexa-594– and Alexa-488–conjugated secondary antibodies (Life Sciences) were used at a final concentration of 1 μg/mL. The coverslips were mounted on glass slides in mounting media (0.5% *p*-phenylenediamine, 20 mM Tris pH 8.8, 90% glycerol). The cells were imaged by epifluorescence on a Nikon TE2000E microscope equipped with an OrcaER camera (Hammamatsu) and 40× PlanApo 0.95NA or 100× PlanApo 1.4-NA oil objective (Nikon). Images were acquired using the Metamorph software (Applied Precision). Ciliary localization of Smo was measured using custom image analysis software implemented in MATLAB. Briefly, the software first identifies cilia by local adaptive thresholding of acetylated tubulin images. The segmented images are cleaned by automatic removal of objects whose size and shape fall outside the normal range for a typical cilium. Next, the pixel intensity of the protein of interest (Smo) in each cilium is corrected by subtracting the local background, defined as the median intensity of the pixels surrounding the cilium. Ciliary Smo is then quantified as the total corrected intensity in each cilium, normalized to the area of the cilium. To count Smo-positive cilia, fluorescence in the Smo channel is first calculated for the cilia in the negative control sample (untreated cells in case of scoring endogenous Smo, or *Smo*$^{-/-}$ cells in case of scoring Cherry-tagged fusions proteins stably expressed in *Smo*$^{-/-}$ MEFs). This data is used to calculate a threshold value that is above the fluorescence intensity for >95% of cilia in the negative control sample; note that this method overestimates the number of Smo-positive cilia in the negative control by allowing a false positive rate of up to 5%. Using the calculated threshold, cilia are then scored in all of the remaining samples, and the fraction of Smo-positive cilia is graphed. The error bars represent the subsampling s.d. of the fraction of positive cilia; this is calculated by dividing the cilia population for each experimental sample into five random and nonoverlapping subsamples, and then calculating the fraction of positive cilia in each subsample and finally calculating the s.d. of the fraction of positive cilia across the subsamples. Smo intensity at cilia is also graphed using box plots; for each condition, the

lower and upper bounds of the box represent the twenty-fifth and seventy-fifth percentile of the Smo intensity distribution, and the horizontal line represents the median intensity across the entire cilia population. For the experiments presented in this paper, between 130–600 cilia were analyzed per condition. For some experiments, ciliary localization of Smo was measured manually by scoring the presence or absence of Smo in 150 cilia per condition.

Sterol depletion. Sterol depletion was performed on starved, confluent cultures of stable lines derived from *Smo*$^{-/-}$ MEFs. The cultures were incubated for 30 min with 1% methyl-β-cyclodextrin (MCD) in DMEM (to remove sterols), after which all subsequent incubations were in DMEM with 20 μM pravastatin (to block new sterol synthesis), with or without the indicated additives. For rescue experiments, cholesterol was added back by incubating the cells for 1 h with soluble cholesterol-MCD complexes (100 μM in DMEM supplemented with 40 μM pravastatin). After overnight incubation with the desired compounds, the cells were processed for immunofluorescence or for quantitative PCR, as described above.

BODIPY-cyclopamine and BODIPY-SANT1 binding assays. Various Smo proteins, tagged at their C termini with Cherry, were expressed in 293T cells either stably or by transient transfection. The cells were incubated for 1 h in DMEM with 10 nM BODIPY-cyclopamine or 10 nM BODIPY-SANT1, in the presence or absence of competitor drug. The cells were washed with DMEM and fixed in PBS with 4% formaldehyde for 20 min, followed by five washes with TBST (10 mM Tris pH 7.5, 150 mM NaCl, 0.2% Triton X-100). The cells were then imaged by epifluorescence microscopy, capturing for each field of view an image of the Smo-Cherry fusion and one of the BODIPY compound.

Preparation of ligand affinity matrices. Free amine derivatives of 22-NHC or 20-OHC were dissolved in dry isopropanol (20 mM final concentration) and were added to amine-reactive Affigel-10 beads (BioRad). After addition of dry triethylamine (100 mM final), the beads were incubated at room temperature overnight with end-over-end rotation. Unreacted sites on the beads were consumed by incubation with ethanolamine (1 M final in isopropanol), after which the beads were washed extensively with isopropanol. The beads were then washed extensively with water, followed by three washes with the wash buffer used in ligand affinity experiments (20 mM HEPES, pH 7.5, 150 mM NaCl, 0.1% dodecyl-β-maltoside). Control beads were generated in parallel by reacting Affigel-10 beads with the ethylene glycol diamine linker (4,7,10-trioxa-1,13-tridecanediamine, 200 mM final) used in the synthesis of 22-NHC or 20-OHC amine derivatives.

Ligand affinity assays. Recombinant protein for ligand affinity assays was produced by stable or transient expression in 293T cells, except for xSmo-eGFP, which was produced in Sf9 cells by baculovirus infection. Cells expressing various transmembrane Smo constructs, C-terminally tagged with Cherry or eGFP, were harvested and lysed on ice for 30 min in lysis buffer (20 mM HEPES, pH 7.5, 150 mM NaCl, 0.5% dodecyl-β-maltoside) supplemented with protease inhibitors (leupeptin, pepstatin and chymostatin at 10 μg/mL final concentration). The detergent extract was clarified by centrifugation at 20,000*g* for 30 min at 4 °C. The supernatant was first incubated with the desired competitor compound or DMSO control for 5 min on ice. All of the compounds were added to binding reactions from DMSO stock solutions. After this incubation, 22-NHC beads, 20-OHC beads or control beads were added, followed by end-over-end rotation for 1 h at 4C. The beads were washed three times with wash buffer (20 mM HEPES, pH 7.5, 150 mM NaCl, 0.1% dodecyl-β-maltoside), after which bound proteins were eluted in SDS-PAGE sample buffer with DTT (50 mM final) at 37 °C. The proteins were separated by SDS-PAGE, followed by immunoblotting with anti-Cherry or anti-GFP (final concentration 1 μg/mL). A portion of the clarified detergent extract was used as input.

Cells expressing HA-tagged secreted SmoCRD constructs were incubated for 48 h in DMEM supplemented with 0.5% FBS, penicillin and streptomycin. The conditioned medium containing soluble SmoCRD protein was harvested, subjected to centrifugation to remove cellular debris and concentrated ten-fold by ultrafiltration through a 10-kDa cutoff concentration device (Amicon). The medium was then supplemented with dodecyl-β-maltoside (0.5% final concentration) and protease inhibitors and was used in ligand affinity assays as described above for detergent extracts of cells expressing full-length Smo proteins.

29. Tukachinsky, H., Lopez, L. & Salic, A. A mechanism for vertebrate Hedgehog signaling: recruitment to cilia and dissociation of SuFu–Gli protein complexes. *J. Cell Biol.* **191**, 415–428 (2010).
30. Tukachinsky, H., Kuzmickas, R.P., Jao, C.Y., Liu, J. & Salic, A. Dispatched and scube mediate the efficient secretion of the cholesterol-modified hedgehog ligand. *Cell Rep.* **2**, 308–320 (2012).
31. Klein, U., Gimpl, G. & Fahrenholz, F. Alteration of the myometrial plasma membrane cholesterol content with β-cyclodextrin modulates the binding affinity of the oxytocin receptor. *Biochemistry* **34**, 13784–13793 (1995).

doi:10.1038/nchembio.1290